Green Synthesis of TiO_2 Nanoparticles and Study of Electrical Properties of TiO_2-Polyaniline Nanocomposites

Kousik Dutta
Assistant Professor in Physics
Department of Physics, Behala College, Parnashree; Kolkata- 700060; INDIA
Author for correspondence: duttakousik2003@yahoo.co.in

Abstract: ***Research is mainly focused on the nature to apply in the field of science and technology, especially in nanotechnology. Aloe Vera plant is oldest herbal medicinal plant as high in vitamins, minerals, amino acids and fatty acid. Green synthesis is a simple, non-toxic, economical and eco-friendly approach for the synthesis of nanoparticles. Biogenic methods of synthesis of nanoparticles (NPs) using plant extracts have been given a great attention due to its nontoxicity and environmental friendliness. Titanium dioxide is an important semiconductor material for wide range of solar energy conversion applications. However, it is limited due to its high bandgap as well as high charge carrier recombination rate under illumination. This can be overcome partly by controlling the size of the particle via green synthesis route using Aloe vera gel extraction. The synthesized particles were characterized using different characterization techniques such as SEM, TEM, XRD. Studies on dc electrical conductivity as a function of temperature suggest that three dimensional Mott's hopping process occurs in TiO_2 – Polyaniline nanocomposites. The correlated barrier hopping is confirmed from temperature dependent ac conductivity. The incorporation of TiO_2 nanoparticles enhances the barrier height.***

Key words : Green Synthesis, TiO_2 nanoparticles, TiO_2-PANI nanocomposites, Electrical properties

I. INTRODUCTION

Nanomaterials belongs to the range of below 100 nm has unique chemical, physical, electrical, and mechanical properties and also diversely utilized in the field of medical, biotechnology, microbiology, pharmaceutics and chemistry, engineering, inexpensive catalyst, cytotoxicity study, etc. **[1]**. Owing to its large surface area, nanomaterial synthesis methods are classified into the physical and chemical methods. However, these methods are not suitable for medicinal and biological applications because of its harmful nature to the environment. Synthesis of nanoparticles taking assistance of green methods has attained enormous attention in the recent years **[2-5]**. Plant systems widely distributed along the ecological boundaries, are easily available and safe to handle. Such studies could prove to have a huge effect in the immediate future, if plant tissue culture and downstream processing procedures are applied in order to synthesize metallic as well as oxide nanoparticles on industrial scale **[6]**. In the past few decades, metal oxide semiconductors such as ZnO, MgO, CuO, CdO, NiO, etc. were widely used, and it is prepared via physical, chemical, and biological methods. Plants attracted few researchers to use their extracts in green synthesis of copper oxide nanoparticles such as Carcia papaya leaf extract **[7]**, Aloe vera leaf extract **[8]**, and Centella asiatica leaf extract **[9]**.

Titanium dioxide (TiO_2) is a naturally abundant metal oxide which occurs in three different forms anatase, brookite and rutile phases **[10]**. TiO_2 NPs are white colored n-type semi-conductor having high thermal stability, excellent optical and dielectrical properties, bio-compatibility and non-toxicity **[11-12]**. Due to these properties TiO_2 NPs are used in vast applications such as photo catalyst, lithium ion batteries, optoelectronic devices, reduction of H_2O_2, solar cells **[13-16]**, etc. Likewise it is also used in sunscreens, pigments, paints, antimicrobial coatings owed to its high refractive index against sunlight [**17]**.

Various methods are applied for the synthesis of TiO_2 NPs such as plasma enhanced chemical vapour deposition, in situ synthesis, sol-gel process, solid state technique **[18-20]** and iosynthesis. Among this methods biosynthesis of TiO_2 NPs get more attention due to its simplicity, non-toxicity, low cost etc **[21]**. Different parts of plants (stem, leaf, flower, peel) are used to control aggregations and agglomerations of the NPs, in which it acts as an oxidizing, reducing and capping agents **[22]**. Green synthesis provides more advantages over physical methods and chemical methods because it is very cost effective, easy process and scalable for large scale production. This method not required high temperatures, high pressure, costly equipment and hazards chemicals. The use of different parts of plants in the biosynthesis of TiO_2 nanoparticles and their applications holds immense potentials towards the environment. The source of the plant extract is known to influence the characteristics of the nanoparticles and hence its applications. This is because different extracts contain different concentrations and different types of organic reducing agents and at same time different capping agents **[23–24]**. Aloe vera, neem, tea, and coffee have been used in synthesis of nanomaterials as a reducing agent to study the effect of variation of morphology or surfactants. **[25]**. Aloe vera has been reported as a good reducing/stabilizing agent for silver nanoparticles **[26]**. The present work green synthesis of TiO_2 nanoparticles is based on the Aloe Vera plant extract. Aloe Vera is oldest medicinal plant ever known and a most applied medicinal plant, which is succulent plant species, the species is frequently cited as being used in herbal medicine since the beginning of the first century AD. Aloe Vera Gel contains a large range of vitamins – even vitamin B12, Vitamin A, contains B-Group vitamins, Vitamin C, Vitamin E, folic acid and amino acids needed by the human body. Aloe vera is a powerful detoxifier, antiseptic, tonic for the nervous system, immune boosting and anti-viral properties, improves digestion.

Table 1

Amount of pyrrole x (ml), room temperature dc conductivity σ (RT), Mott's parameters of Eq. (2) σ_0 and T_0 density of states $N(E_F)$, hopping length R_{hop}, barrier height W_{hop}

Sample	X ml	σ (RT) (10^{-3} S/cm)	σ_0 (10^3 S/cm)	T_0 (10^6 K)	N_{EF}($eV^{-1}cm^{-3}$)	R_{hop} (A)	W_{hop} (meV)
S1	0.35	0.75	2.25	12.75	1.52	23.12	135
S2	0.50	0.90	0.95	4.75	3.21	20.34	121
S3	0.65	1.25	0.10	0.95	8.55	15.35	105

Polyaniline is the most attractive conducting polymers because of its low cost, high environmental stability, good electrical conductivity, and potential applications in molecular electronics **[27]**. The electrical properties of polymers can be modified by addition of inorganic fillers. Nanoscale particles are more attractive due to intriguing properties arising from nanosize and large surface area. The insertion of nanoscale fillers may improve the electrical properties of the host polymers. Polymer-semiconductor nanocomposites generate a new field for the development of advanced materials in science and technology **[28]**. The properties of nanocomposites are quite different from the constituent materials due to interfacial interactions between nanostructured semiconductors and polymers. In this work it is reported that the transport properties of PANI-TiO_2 nanocomposites at low temperature and high frequency.

II. MATERIALS AND METHODS

All the chemicals were of analytical grade and purchased from Merck (India) and used without further purification. Aniline (AR grade) was purified and stored at -15^0C in a refrigerator prior to use. APS oxidant was used as received and de-ionized water was employed for preparing all the solutions and reagents. The

samples were characterized by x-ray powder diffraction patterns employing a scanning rate of 0.02 0 per 2 sec in 2θ range from 20 to 70 using a Philips (PW1710) x-ray diffractometer equipped with monochromatized Cukα radiations. Morphological studies were performed with JEOL JSM6700F Scanning electron microscope (SEM). Transmission electron micrograph (TEM) was taken from JEOL, JEM 2010 with acceleration voltage of 200 KV. The electrical contacts were made by silver paint on both sides of the sample. Dry powdered sample were made into pellets using a steel die of 1 cm diameter in a hydraulic press under a pressure of 5 ton. The thickness of the samples varies from 0.04 cm to 0.08 cm. For electrical measurements the electrical contacts were made by silver paint.

A. Preparation of aloe Vera leaf extract

Fresh and healthy Aloe Vera plant was collected locally. One of the selected leaves was cut and washed twice with tap water followed by distilled water to remove dust particles and other contaminants. 50g of the leaves was weighed using electronic weighing balance and transferred into a 500 ml beaker containing 200 ml distilled water. The contents were boiled for 4h at 75°C. The extract was filtered using Whatman filter paper. The filtrate was stored for the synthesis of nanoparticles.

B. Synthesis of Titanium Oxide (TiO_2) nanoparticles by aloe Vera leaf extract

To synthesis the TiO_2 nanoparticles, dissolve 1.0 N of Titanium Chloride ($TiCl_4$) in 100 ml of Millipore water. Added leaves extract drop wise under constant stirring up to achieve pH of solution became 7. The mixture was subjected to stirring for 4 hours continuously. The NPs formed during the process were collected by centrifugation (10,000 rpm) and repeatedly washed with ethanol (absolute). to remove the byproducts. The nanoparticles were dried at 100°C for overnight and calcined at 500°C for 4 hours.

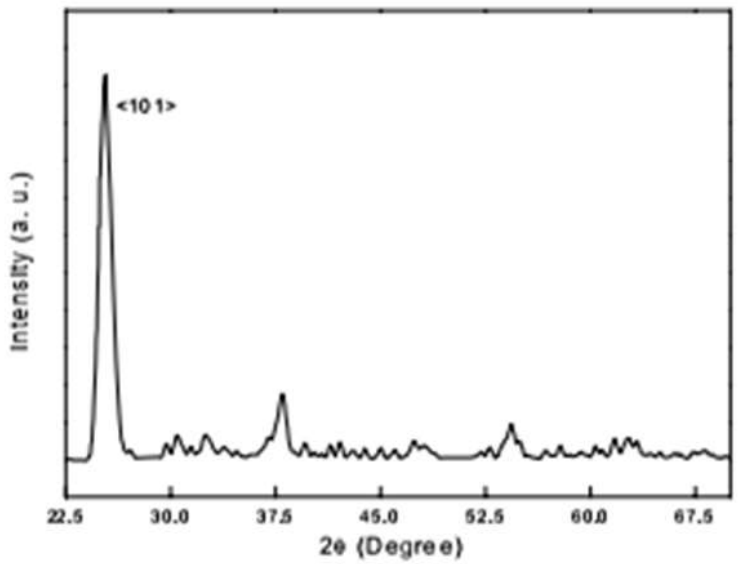

Figure 1: X-ray diffraction pattern of PANI-TiO_2 nanocomposite sample S1.

C. Synthesis of TiO_2 - PANI nanocomposite

The required quantity of TiO_2 nanoparticle was ultrasonically dispersed in 50 ml deionized water. Aniline monomer of known volume was slowly added into the dispersion under sonication at room temperature. Then the aqueous solution of APS maintaining a pyrrole : APS mole ratio of 1:1.25 was added drop wise into the previous solution. After few hours the resulting solution

was turned into green color which indicates the formation of polyaniline. The solution was then kept under sonication for about 10 hours to ensure complete polymerization. Finally, the resulting green dispersion were centrifuged. The resulting nanocomposites were washed thoroughly with distilled water for several times. Different compositions of nanocomposite samples by varying the weight percentage of aniline(polyaniline) were prepared as shown in Table I.

III. RESULTS AND DISCUSSION

Fig. 1 shows the characteristic peaks of X-ray diffraction (XRD) of the sample S1. The spectra reveals the presence of anatase phase of Titania in the nanocomposites. The crystallite size of the TiO_2 nanoparticles in the composite sample S1 is calculated following the Scherrer's relation (using 101 face) **[29]**

$$D = K\lambda/\beta\cos\theta \quad \textbf{(1)}$$

where K=0.89, D represents crystallite size (nm), λ, the wavelength of CuKα radiation and β, the corrected value at half width of the diffraction peak. At $2\theta=25.36^{o}$ (101), which is the characteristics peak of TiO_2, is chosen to calculate the average diameter and it comes out to be 25 nm, which is consistent with that obtained from TEM studies.

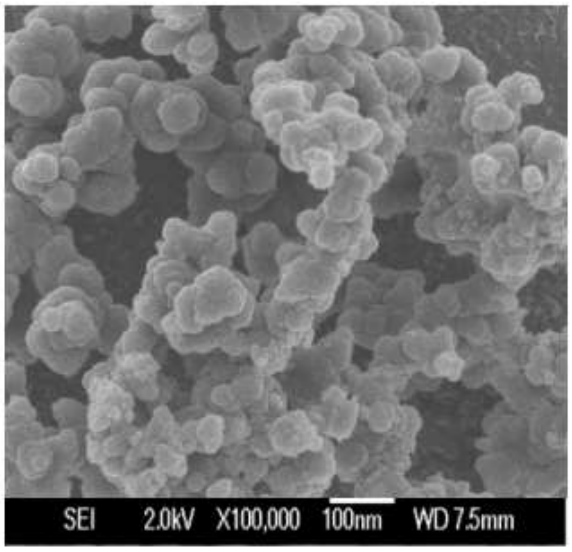

Figure 2: Scanning electron micrograph of sample S1.

The scanning electron micrograph (SEM) of the nanocomposite sample S1 is shown in Figure 2. The TiO_2 nanoparticles are well dispersed and are of spherical in shape with uniform diameter lying in the range from 25- 30 nm. Larger particle size may be due to the aggregation of smaller particles in the presence of polymer matrix.

Figure 3. shows the TEM micrograph of the TiO_2 – polyaniline nanocomposite S1 sample. In this micrograph nearly, spherical crystallites are observed. The mean particle size of pure TiO_2 is in the range of 15-20 nm. Larger particle size due to the aggregation of smaller particles in the presence of polymer matrix. The nano particles are polydispersed and are of spherical shape with uniform diameter lying in the range from 20-25 nm. After the formation of the composites the particles are found to be entrapped into polyaniline chains. Immediate conclusion is that the colloid particles are not simply mixed up or blended with the polymer, they are rather encapsulated by the polyaniline chains.

Figure 4 shows the FTIR spectra of polyaniline (PANI) doped with HCl and PANI-TiO_2 nanocomposite samples S1, S2 and S3 respectively. The characteristics peaks of HCl doped PANI are assigned as follows. The band at 1560 and 1474 cm^{-1} are attributed to C=N and C=C stretching mode of vibration for the quinonoid and benzenoid units, while the bands at 1303 and 1242 cm^{-1} are assigned to C-N stretching mode of benzenoid units. The band at 1108 cm^{-1} is due to quinonoid unit of doped PANI. The peak at 795 cm^{-1} is attributed to C-C and C-H for benzenoid unit. The incorporation of TiO_2 in the nanocomposites leads to small shift of some FTIR peaks in PANI.

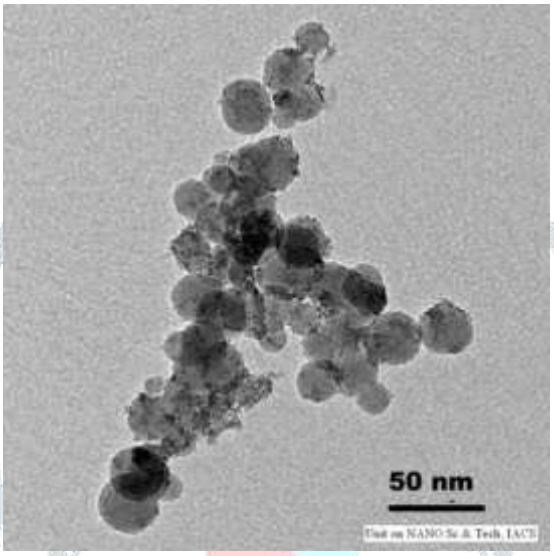

Figure 3: Tunneling electron micrograph of sample S1.

The dc conductivity σ(RT) at room temperature for various compositions are shown in Table I. The weight percentage of conducting PANI is much higher than 13 % of classical percolation threshold. As a result of it the conductivity does not change significantly with the increase of conducting PANI fraction. The temperature dependence of conductivity for three different compositions

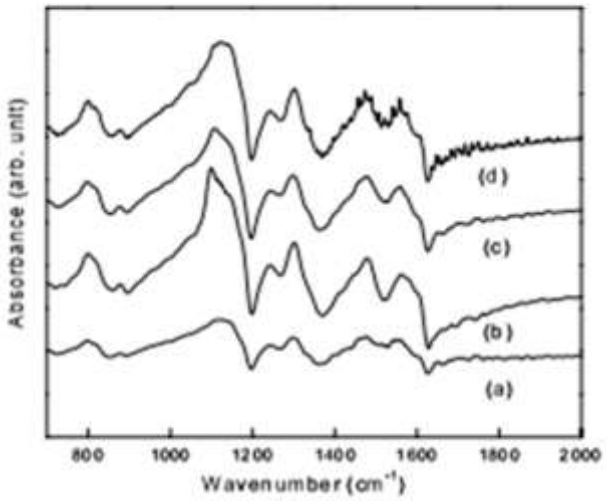

Figure 4: Fourier Transform Infrared (FTIR) spectra of (a) HCl doped PANI (S4) (b) nanocomposite S1 (c) nanocomposite S2 and (d) nanocomposite S3.

are shown in Figure 5. The conductivity increases with increases of temperature which is the characteristic behavior of semiconductors. The temperature dependence of conductivity $\sigma(T)$ of disordered semiconducting materials is generally described by the Mott's variable range hopping (VRH) model, **[30]**

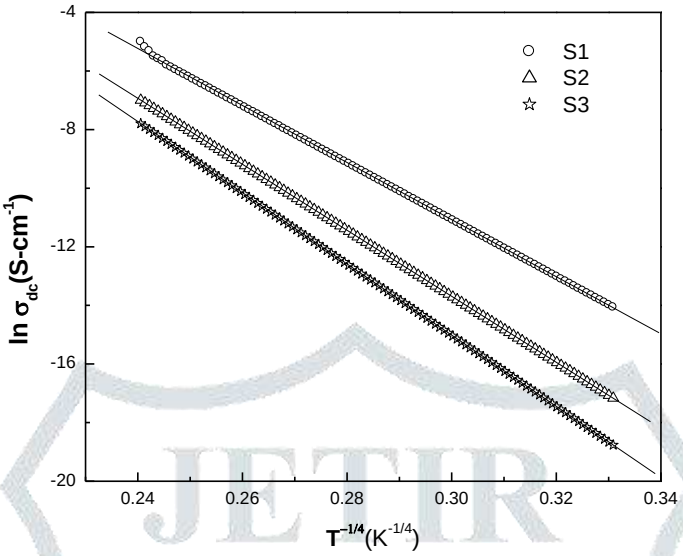

Fig. 5. Temperature variation of dc conductivity of the nanocomposites S1, S2, and S3 respectively. The solid lines are fit to Eq. (2)

$$\sigma(T) = \sigma_0 \exp\left(-(T_0/T)^{\gamma}\right) \quad \textbf{(2)}$$

where σ_0 is the high temperature limit of conductivity and T_0 is Mott's characteristic temperature associated with the degree of localization of the electronic wave function. The exponent $\gamma = 1/(1+d)$ determines the dimensionality of the conducting medium. The possible values of γ are 1/4, 1/3 and 1/2 for three, two and one dimensional systems respectively. The plot of ln $\sigma(T)$ against $T^{-1/4}$ indicates that three-dimensional (3D) charge transport occurs in all the samples. The values of Mott's characteristic temperature T_0 and the pre exponential factor σ_0 are obtained from the slopes and intercepts of the Figure. 5 and are given in Table I. The values of T_0 are very sensitive and decrease with increasing PANI content. Both PANI-TiO_2 nanocomposites and pure PANI follow three dimensional VRH electrical conduction process.

Titania is a wide band gap (3.2 eV) semiconductor. It does not contribute to electric conduction at low temperature. The ionic conduction only arises at high temperature due to the extrinsic ionic defects. The conducting component of the nanocomposite is polyaniline. The polymerization of aniline monomer occurs on the surface of Titania nanoparticles. The monomer associated with nanoparticles decreases with decrease of monomer content. This reduces the conjugation length and conductivity of polyaniline. The presence of insulating Titania regions also dominant at high Titania content. Hence the conductivity of nanocomposite decreases with increase of Titania content.

The characteristic temperature T_0 for three dimensional hopping transport is given by,

$$T_0 = 16/\left(kL^3 N(E_F)\right), \quad (3)$$

where k is Boltzmann constant where L is the localization length and N(EF) is the density of states at the Fermi level. Eq. (3) indicates that T_0 depends on both the localization length (L) and density of states ($N(EF)$). The

observation of three dimensional hopping process suggests that the charge transport primarily arises from conducting PANI phase. The density of states, *N(EF)* are calculated by assuming localization length of the aniline monomer unit about 3 Å, i.e. L = 3 Å, in Eq. (3). The estimated values of *N(EF)* increase with the amount of aniline monomer. The enhancement of *N(EF)* increases the hopping probability between the localized states. This is also consistent with the increase of dc conductivity with increase of aniline content.

The average hopping distance R_{hop} between two sites and the barrier height W_{hop} are

$$R_{hop} = (3/8)(T_0/T)^{1/4}L,$$
$$W_{hop} = (1/4)kT(T_0/T)^{1/4}. \qquad (4)\ \&\ (5)$$

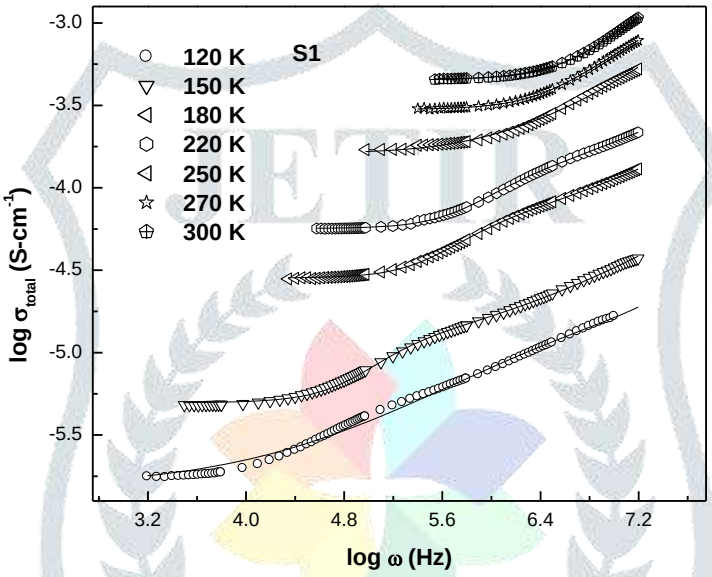

Figure 6. Frequency dependence of conductivity at different temperatures of the sample S1

At room temperature the average hopping distance for sample S1 is about 23 Å, and it reduces to about 15 Å, for the highest content of aniline. This corresponds to about 8–5 monomer units in length. The estimated barrier heights for hopping as shown in Table 1 are in the range of 135–105 meV. Both the hopping distance and barrier height decreases as conductivity increases. The closer approaches of hopping sites enhances the conductivity.

The ac conductivity of samples S1, S2 and S3 are investigated. The variations of ac conductivity $\sigma(\omega)$ as a function of frequency at different temperatures are shown in Figure. 6 for the sample S1. The plateau observed in $\sigma(\omega)$ at low frequency correspond to dc conductivity. The conductivity starts to increase from dc value after certain characteristic frequency ω_0 known as cross over frequency. The plateau region is more with increasing temperature. The extra contribution to conductivity comes from capacitive regions which provide less impedance at higher frequency. Figure 6 reveals that ω_0 is strongly temperature dependent

A general feature of amorphous semiconductors and disordered systems is that the frequency dependent conductivity $\sigma(\omega)$ obeys a power law with frequency. The total

conductivity $\sigma(\omega)$ at a particular temperature over a wide range of frequencies can be expressed as

$$\sigma(\omega) = \sigma_{dc} + A\omega^S \quad (6)$$

where σ_{dc} is the dc conductivity and A is a constant dependent on temperature. The frequency exponent S lies between 0 and 1 and is given by S = d $ln\sigma(\omega)$/ d $ln\ \omega$. The value of S at each temperature has been calculated from the slope of log [$\sigma(\omega)$- σ_{dc}] vs log ω plot. The estimated values of S are between 0.1 and 0.65 for S1 samples as shown in Figure 7.

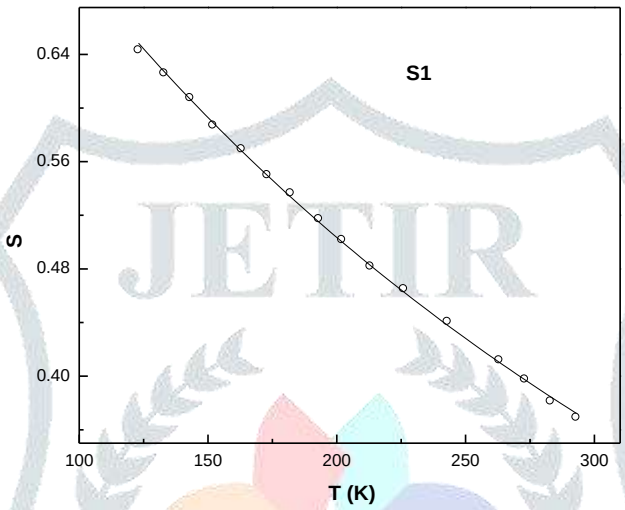

Fig. 7. Frequency exponent (*S*) vs. temperature (*T*) for the samples S1. The solid lines are fit to Eq. (7)

The microscopic conduction mechanisms of disordered systems are governed by two physical processes such as classical hopping and quantum mechanical tunnelling of charge carries over the potential barrier seperating two energetically favorable centres in a random distribution. The exact nature of charge transport is mainly obtained experimentally from the temperature variation of exponent S. Temperature dependence of S for S1 samples are shown in Figure. 7. The value of frequency exponent S decreases with increase of temperature. This behavior is only observed in correlated barrier hopping model [31]. The temperature dependence of S based on this model is

$$S = 1 - \frac{6kT}{W_M - kTln(\frac{1}{\omega\tau_0})} \quad (7)$$

where W_M is the effective barrier height at infinite intersite separation, τ_0 is the characteristic relaxation time and k is the Boltzmann constant. The values of W_M and τ_0 are obtained by the best fitted parameters to Eq 7. at a frequency of 100 KHz and are given in Table 2. Fig. 7 exhibits that the experimental values of S are in good agreement with theoretical model.

Table 2

Best fitted values of W_M , τ_0 R_ω of Eq. (7) & (8)

Sample	W_M (meV)	τ_0 (10^{-6} s)	R_ω (10^{-2} A^0)
S1	130	7.50	1.05
S2	119	0.55	7.50
S3	101	0.03	11.54

The hopping distance (R_ω) at a particular frequency and temperature is [**31**]

$$R_\omega = \frac{e^2}{\pi\epsilon\epsilon_0}[W_M - kTln(\frac{1}{\omega\tau_0})] \quad (8)$$

where e is the electronic charge, Ɛ and $Ɛ_0$ are dielectric permittivity of material and free space respectively. The calculated hopping distance for different samples are shown in Table 2. The value of (R_ω)increases with increasing PANI content.

The expression for ac conductivity in correlated barrier hopping model is

$$\sigma_1(\omega) = \frac{1}{24}\pi^3 N^2 \epsilon\epsilon_0 \omega R_\omega^6 \quad (9)$$

where N= kTN(*EF*), and N(*EF*) is the density of states at Fermi level. The best fitted values of W_M and τ_0 are used to calculate N(*EF*) from equation 9. With increasing PANI content density of states decreases which indicate the existence of delocalized electronic states.

IV. CONCLUSION

Titania nanoparticle affects the energy interval between the highest occupied and the lowest unoccupied states of polyaniline. Conducting polyaniline plays a key role in determining the transport mechanisms of nanocomposites. Three-dimensional variable range hopping conduction is observed in dc charge transport. Ac conductivity reveals correlated barrier hopping type conduction process. The barrier height decreases with increase of polyaniline concentration.

V. RRFERENCES

[1] Hemalatha K, Madhumitha G, Kajbafvala A, Anupama N, Sompalle R, MohanaRoopan S (2013) J Nanomater 2013:341015.

[2] Chandran S.P., Chaudhary M., Pasricha R., Ahmad A., Sastry M. (2006), Biotechnol. Prog. 22, 277-583.

[3] Jafarirad S., Mehrabi M. and Pur E.R. (2014), Biomedical and Environment Engineering. 62-64.

[4] Raveendran P., Fu J., Wallen S.L. (2003), J. Am. Chem. Soc. 125, 13940–13941.

[5] Kalimuthu K., Babu R.S., Venkataraman D., Mohd B., Gurunathanm S. (2008), Colloids Surf. B 65, 150–153

[6] Suresh Y., Annapurna S., Singh A.K., Bhikshamaiah G. (2014), International Journal of Innovative Research in Science, Engineering and Technology. 3(4), 11265-11270

[7] Sankar R., Manikandan P., Malarizhi V., Fathima T., Shivashangari K.S., Ravikumar V. (2014) Spectrochimica Acta A: Molecular and Biomolecular Spectroscopy. 121, 746-750.
[8] Gunalan S., Sivaraj R., Venckatesh R. (2012) Spectrochimica Acta A: Molecular and Biomolecular Spectroscopy. 97, 1140-1144.
[9] Devi H.S., Singh T.D. (2014) Advance in Electronic and Electric Engineering. 4, 83-88.

[10] Rajneesh Mohan, Jana Drbohlavova and Jaromir Hubalek, Nanoscale Research Letters. 8(1) (2013) 4.
[11] Fox M.A, Dulay M.T, Chem. Rev. 93 (1993) 341–357.
[12] Varahalarao Vadlapudi, 173 I J P A C. 9 (2014) 167.
[13] L. Gomathi Devi, Nagaraju Kottam, B. Narasimha Murthy, S. Girish Kumar, Journal of Molecular Catalysis A. 328 (2010) 44–52.
[14] Reddy C.Raghu, Rao R.N and Prakash1 T.L, Archives of Applied Science Research. 4 (3) (2012) 1528-1531.
[15] Low C.T.J., Leon C. Ponce de, Walsh F.C., J. Electrochem. 44 (2013) 169–177.
[16] Prabu K.M., Anbarasan P.M., International Journal of Science and Research (IJSR). 3 (2013) 132-137.
[17] Shaw T., Simpson B., Wilson B., Oostman H., Rainey D., Dermatitis Storrs F 21 (4) (2010) 185–98.
[18] Yoshiki Hiroyuki, Mitsui Toshiaki, Surface & Coatings Technology. 202 (2008) 5266–5270
[19] Timothy N. Lambert, A. Carlos, Chavez, Bernadette Hernandez-Sanchez, Ping Lu, Nelson S. Bell, Andrea Ambrosini, Thomas Friedman, Timothy J. Boyle, David R. Wheeler and Dale L. Huber, J. Phys. Chem. C 113 (2009) 19812–19823.
[20] Lo´pez Rosendo, Go´mez Ricardo, J. Sol-Gel Sci Technol. 61 (2012) 1–7.
[21] Abbas S.M., Dixit A.K., Chatterjee R., Goel T.C., Mater.Sci. Eng. B 123 (2) (2005) 167–171.
[22] Rai M., Gade A. and Yadav A., Springer-Verlag Berlin Heidelberg. (2011) 12-26.

[23] Baker S., Rakshith D., Kavitha K. S. et al., Bioimpacts, vol. 3, no. 3, pp. 111–117, 2013.
[24] Mukunthan K. S. and Balaji S., International Journal of Green Nanotechnology, vol. 4, no. 2, pp. 71–79, 2012.
[25] Holmberg K. (2001). *Curr. Opin. Colloid Interface Sci.*, 6: 148–159.
[26] Ibrahim S., Fadhil A. M. A., & AlAni, N. K. (2014). *J. Al-Nahrain Univ. Sci*., 17: 165–171.

[27] Skothemin T., Elsenbaumer R., *Handbook of Conducting Polymers*, Marcel Dekker, New York, 1998.

[28] Nalwa H. S. (editor) Handbook of Organic-Inorganic Hybrid Materials and Nanocomposites, Chapter H-Conducting Polymer Nanocomposites, R. Gangopadhyay and A. De. (American scientific Publishers, 2003).

[29] H. P. Klug and L. E. Alexander, X-ray diffraction procedures for polycrystalline and amorphous materials, John Wiley and Sons, New York, 1954, p491.
[30] Mott N.F, Davis E., Electronic Process in Non-Crystalline Materials, second ed., Clarendon, Oxford, 1979.

[31] Elliott S.R., Adv. Phys. 37 (1987) 135.